

The DLR Hand Arm System

Markus Grebenstein and Alin Albu-Schäffer, Thomas Bahls, Maxime Chalon, Oliver Eiberger, Werner Friedl, Robin Gruber, Sami Haddadin, Ulrich Hagn, Robert Haslinger, Hannes Höppner, Stefan Jörg, Mathias Nickl, Alexander Nothhelfer, Florian Petit, Josef Reill, Nikolaus Seitz, Thomas Wimböck, Sebastian Wolf, Tilo Wüsthoff, and Gerd Hirzinger

Email: Markus.Grebenstein@dlr.de

Institute of Robotics and Mechatronics, German Aerospace Center, Germany

Abstract—An anthropomorphic hand arm system using variable stiffness actuation has been developed at DLR. It is aimed to reach its human archetype regarding size, weight and performance. The main focus of our development is put on robustness, dynamic performance and dexterity. Therefore, a paradigm change from impedance controlled, but mechanically stiff joints to robots using intrinsic variable compliance joints is carried out.

Collisions of the rigid joint robot at high speeds with stiff objects induce the energy too fast for an active controller to prevent damages. In contrast, passively compliant robots are able to temporarily store energy. In this case the resulting internal forces applied to the robot structure and the drive trains are reduced. Furthermore, the energy storage allows to outperform the dynamics of stiff robots.

The hand drives and the electronics are completely integrated within the forearm. Extremely miniaturized electronics have been developed to drive the 52 motors of the system and interface their sensors. Several variable stiffness actuation principles used in the arm joints and the hand are presented. The paper highlights the different requirements that they have to fulfill. A first test of the systems robustness and dynamics has been performed by driving nails with a grasped hammer and is demonstrated in the attached video.

I. INTRODUCTION

Starting point of this research is the insight that a humanoid robot system has to operate in hard-to-predict environments and, by this, collisions with other objects are most likely inevitable. Nevertheless, withstanding collisions and impacts without severe damage or functional impairment is paramount to the successful and reliable completion of a task. The dynamical capabilities of the latest robot generations are not yet sufficient for several tasks. In cyclic tasks (running or bouncing) or in highly dynamic tasks (throwing) the actuators can not provide enough energy during peak loads without getting too bulky and heavy.

An typical example of the shortcomings of robotic hardware robustness is the DLR ball catching demonstration. The combination of the DLR LBR III and Hand II produces a maximum fingertip force of 30 N. However it reaches its mechanical limits catching a ball of only 80 g which hits the fingertip at a speed of 25 km/h. In contrast, a handball goalkeeper withstands the impact of a 480 g ball at 120 km/h which introduces more than 100 times higher energy [1].

Well-known humanoid robots like Honda's Asimo [2] or the HRP 2 developed by Kawada Industries [3] are two impressive examples of robots with rigid joints and links. There exist several humanoid systems that introduced serial elastic actuators. The Waseda robot Wendy [4] is the first humanoid with slowly adjustable mechanical joint stiffness. In the subsequent version, TwendyOne, the adjustability was removed in order to save space in the arms [5].

Robonaut R2 [6] recently presented by NASA also contains serial elastic actuators. It is equipped with dexterous hands that are remotely actuated from the forearm. The humanoid Kenta was developed with a tendon driven spine [7] and more recently the robot Kojiro was built with 109 tendon drives [8]. Beside these humanoid systems, bio-inspired robotic hands replicating the human hand closely have been proposed. The anatomically correct testbed (ACT) Hand [9] and the Shadow Dexterous Hand are both tendon driven hands. The ACT Hand focuses on the one-to-one copy of the human tendon kinematics. The design of serial elastic actuators requires a trade-off between robustness and task performance. In order to avoid this tradeoff, several variable stiffness actuators have been proposed [10], [11], [12], [13], [14].

Human joints are actuated antagonistically. Every degree of freedom (DoF) has an agonist and an antagonist muscle. This is inevitable since human muscles are only able to produce tensile force. Since the muscles, tendons and ligaments are compliant having nonlinear stiffness characteristics, the human is able to adjust the joint stiffness a priori by activating agonist and antagonist simultaneously. Therefore, especially in known or predictable situations, the human is able to adapt his stiffness to prepare for impact.

In humans, the elasticity provided by the muscles, tendons and ligaments decouples the link position from the drive position (see also section III) by storing energy. Generally speaking, the energy introduced into the system, no matter whether caused by a collision, external forces or acceleration of the link inertia is converted to elastic energy. This power source can be used to regain kinetic energy and therefore enhance the dynamics of the system.

To improve positioning accuracy most robots are currently

built as stiff as possible. Compliance of these *stiff robots* is, in most cases, realized using impedance control [15]. Impedance control enables an "active compliance" by means of a feedback controller running at a specific sampling rate. Therefore, the physical stiffness of the robot equals its mechanical stiffness at least during the first control cycle. To reach the desired compliance the inertia of the robot and in particular the drives need to be accelerated to desired position and speed. Haddadin [16],[17] has shown that the peak load during impact of the impedance controlled DLR LBR III¹ occurs too fast to be measured in time by the joint torque sensors. Consequently, any *stiff robot* using "active compliance" appears stiff in case of collision.

In [13], Wolf shows that the actuation systems used within the DLR Hand Arm System can produce a link speed 2.6 times the drive speed using the energy stored in the elastic elements. In case of collision the decoupling of drive and link, through to energy storage, results in lower peak torques on the drives. *Stiff robots* can not store energy². Therefore, any externally introduced energy has to be dissipated actively by the drives.

The main contributions of this paper are: The presentation of the novel anthropomorphic DLR Hand Arm System with variable stiffness actuation. Based on various variable stiffness joints the dynamic motion capabilities and robustness w.r.t. collisions were realized for a complete dexterous hand arm system. The deep integration of the necessary mechanics and electronics to realize variable stiffness actuation into the restricted space is another key challenge of this work. Furthermore, preliminary experimental results confirm our design concept. As a consequence the robot will foster the development of more dynamic robotic applications.

Another contribution is the consequent design methodology to derive anthropomorphic robots from biology: Since the spread between biological and technical systems is very large, the key to a robust and highly dynamic hand arm system is to understand the human in a functional way rather than seamlessly trying to copy it. This prevents from copying its drawbacks to the technical system, rather than only the assets of the biological solution [18], [19], [20].

In a first section a short overview of the system and the used variable stiffness actuation principles and the underlying requirements that drove the decision to use these is given. The mechanical design of the arm, forearm, wrist and hand as well as the realization of the drives is outlined in the second section followed by a short description of the controller design of the arm and the hand. An overview of the software and electronics, developed to enable the high grade of integration and to reduce system complexity, closes the description of the DLR Hand Arm System. First results achieved with the robot conclude the paper.

II. MECHANICS

The DLR Hand Arm System (Fig. 1) mimics the kinematic, dynamic and force properties of the human arm using

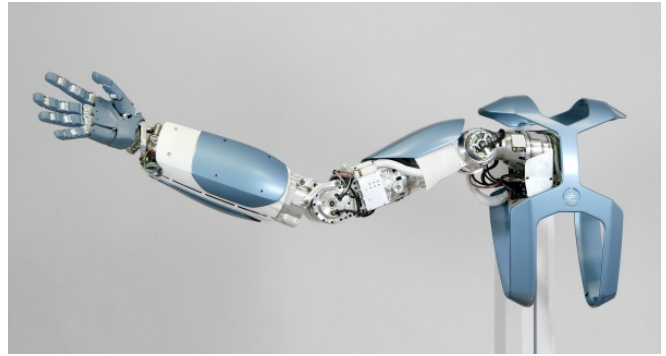


Fig. 1. DLR Hand Arm System

variable stiffness actuation within all joints of the arm and the hand (see Table I)³.

TABLE I
VELOCITIES AND TORQUES OF THE JOINTS

| Joint | Arm | Forearm rotation | Wrist | Finger base | Finger 2nd | Finger 3rd |
|----------------|-----|------------------|-------|-------------|------------|------------|
| Velocity [°/s] | 530 | 960 | 560 | 600 | 960 | 1280 |
| Torque [Nm] | 67 | 8 | 8 | 2.73 | 1.57 | 0.93 |

A. Drive Principles

Since actuation requirements of the arm and the hand differ significantly, different drive principles have been implemented (Fig. 2). Please note that the joint torque measurements are performed using the torque-displacement relationship of the elastic elements in the joints. No further torque sensing device is necessary.

This section shortly presents the different mechanisms of the DLR Hand Arm System.

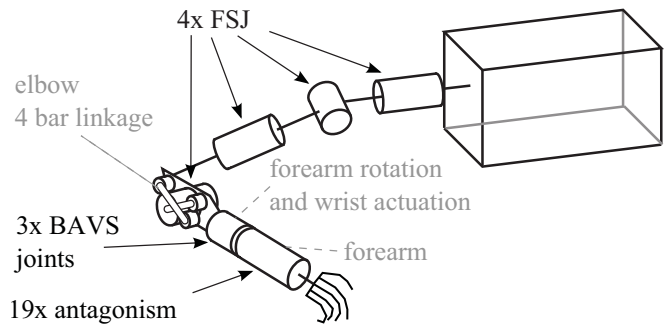


Fig. 2. Location and name of the drive principles.

Vibration damping and low friction within the joints especially in the shoulder is crucial for the performance and accuracy of the arm. Therefore, the newly developed DLR Floating Spring Joints (FSJ) [21] are used within the first 4 axes of the arm to enable precise motion.

The space available for the drives of the wrist joints and the forearm rotation is limited by the forearm length.

¹Impact between a DLR LBR III and a crashtest dummy.

²Neglecting the rather small elasticity of standard robot joints.

³all velocities are maximum drive speeds. Joint/link speeds relate to the amount of stored energy

However, the drives need high power density to carry the torques resulting from the finger tendon loads at the wrist⁴. For this special requirement, the Bidirectional Antagonistic Variable Stiffness (BAVS) joint was designed.

Finally, for the fingers, vibration damping is of limited relevance⁵. Nonetheless, the drives have to fulfill the specific requirements of tendon actuation (see II-E) and shall be as compact as possible in order to fit into the forearm.

Moreover, to reduce system complexity the drive components should be modular and easily exchangeable. Following those requirements, the antagonistic drive principle with a variable stiffness element in the tendon path was chosen for the hand actuation.

Floating Spring Joints (FSJ)

The FSJ is a variable stiffness joint with one dominant motor for joint positioning. The motor to change the stiffness (see Fig. 3) is much smaller, assuming that the stiffness preset is not changed rapidly and persistently during a trajectory.

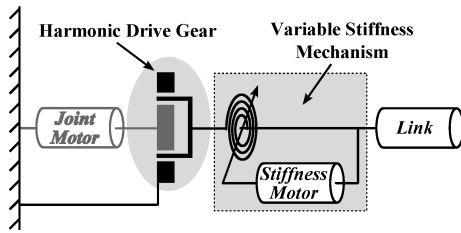


Fig. 3. The variable stiffness mechanism of the FSJ is located in series between the harmonic drive gear box of the main actuator and the link.

Antagonism

Antagonism is characterized by two actuators and two elastic elements for each DoF which exert in analogy to the human archetype only unilateral forces. They move the link when driven in the same direction and alter stiffness when driven in opposing directions (Fig. 4).

Since antagonism uses only one torque direction of the motors, the maximum torque applicable is the maximum motor torque. Therefore, antagonism is not optimal regarding force to weight/size ratio.

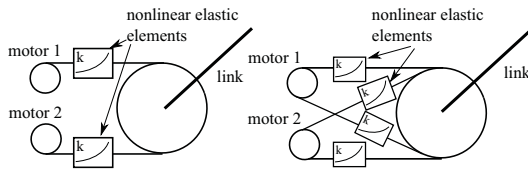


Fig. 4. Antagonism and BAVSdrive principle.

Bidirectional Antagonistic Variable Stiffness Joints (BAVS)

To eliminate the drawback of classical antagonism the Bidirectional Antagonistic Variable Stiffness (BAVS) joints (BAVS) [22] [23] were developed (Fig. 4). To use the combined motor torques, both motion directions of the motor transfer actuation forces. For tendon actuation, the number of

⁴It is impossible to route all the tendons through the instantaneous rotation center of the wrist to produce no net wrist torque.

⁵finger dynamics are negligible w.r.t the respective friction forces

necessary tendons doubles (Fig. 4). Therefore, the integration of BAVS-actuation into the desired hand is not possible. However they are very well suitable for the wrist joint and forearm rotation.

B. Arm

The arm consists of a 3 DoF shoulder and a 1 DoF elbow in a serial kinematics chain (Fig. 2).

The FSJ mechanics (Fig. 5) is a derivation of two previous joint prototypes developed at DLR: the VS-Joint [13] and the QA-Joint [24]. Analogue to the VS-Joint the torque is generated via a rotational cam disk and roller system, which transmits the rotational joint deflection to an axial compression of a linear spring. The shape of the cam disks can be chosen freely in order to gain the desired stiffness characteristics.

The two cam disks of the DLR FSJ are coupled with each other by a single linear "floating spring"⁶. The "floating spring" is directly connected to the two cam disks and compresses them axially. A pair of cam rollers located between the cam disks is attached to the main drive unit. An increasing deflection of the rollers with respect to the cam disks unit generates a progressive restoring torque due to the compression of the spring and the cam disk curvature (Fig. 5c). Relative motion of the cam disks with respect to each other changes the stiffness of the joint (Fig. 5a,b). The "floating spring" mechanism enables the use of a high energy spring in a very compact package. [21]

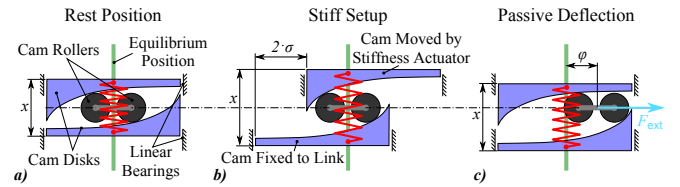


Fig. 5. Unwound principle of the FSJ mechanism. A pair of cam rollers located between the cam disks is directly attached to the harmonic drive gear output of the main motor, axially and radially guided by a bearing. The spring is compressed/elongated by a rotational relative movement of the cam disks, as well as by rotational movement of the roller base with respect to both cam disks. The axial force of the compressed spring results in opposing tangential forces that depend on the spatial gradient of the cam disks and the spring compression. a) and b) The joint stiffness can be changed by twisting the cam disks relatively to each other. c) The stiffness characteristics at a given stiffness preset is a result of the "floating spring" compression due to passive deflection and both cam disk gradients.

C. Forearm

Logically the forearm can be divided into two sections. The forearm rotation joint, which is a separate structure and the forearm itself to actuate the 2-DoF wrist and 19-DoF hand. All 42 motors and 42 nonlinear compliance mechanisms had to be integrated into the forearm (Fig. 6). Each compliance element is adapted to the different finger and joint characteristics. Further fast replacement of the motor modules (ServoModules) and tendons is helpful for maintenance reasons. Each ServoModule contains the motor,

⁶the spring is neither connected to the joint base nor to the output shaft

the position sensors, the electronics, and the wave generator of the harmonic drive gear (HD) (Fig. 14). Due to the compact packaging of the electronics and the power density of the motors, the generated thermal energy exceeds the technical limits of typical air cooling systems. Using a water cooling system the heat can effectively be transferred out of the system. These requirements consequently led to a split forearm design.

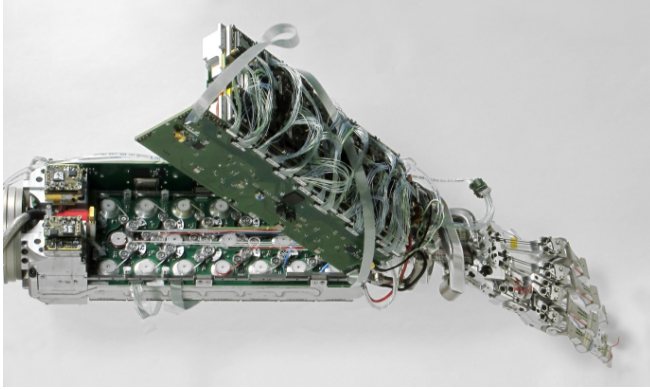


Fig. 6. Forearm with ServoModules. The ServoModules are located on the outside of each half. The tendons and elastic elements are located in the middle layer between both halves. This design of the forearm-structure has several benefits, such as protecting the tendons in the middle of the forearm. Furthermore, all ServoModules are easy to reach and to replace. To replace a ServoModule only two screws have to be released and the low level bus connector has to be disconnected.

a) *Actuation of the Fingers:* The fingers are actuated via the ServoModules. A multiturn winder transfers the rotational gear motion to the tendons. The compliance mechanism is similar to the one described in [18]. One difference is that the winder also acts as the first pulley of the "tan α mechanism" (Fig. 7). This reduces the number of required pulleys.

The characteristics of every finger joint can be adapted by selecting the equilibrium point, the spring rate and the spring position. The tendon length and its serial elasticity need to be modeled to appropriately design the target "stiffness to deflection characteristics".

b) *Actuation of the Wrist and Forearm Rotation:* The requirements for the wrist and forearm rotation actuators are almost identical. Therefore, the compact ServoModules were used for both in slightly modified versions. The required

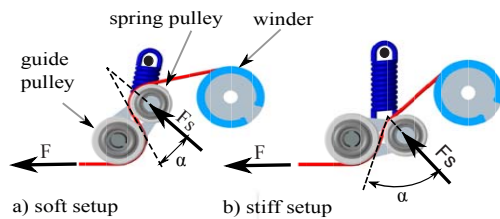


Fig. 7. Antagonistic drive compliance mechanism ("tan α mechanism"): The pulley located at the spring loaded lever rotates around the center of the guiding pulley. Due to this design, a non-linear relation between tendon force and spring elongation is obtained. a) low mechanical stiffness due to small α b) large α results in high stiffness.

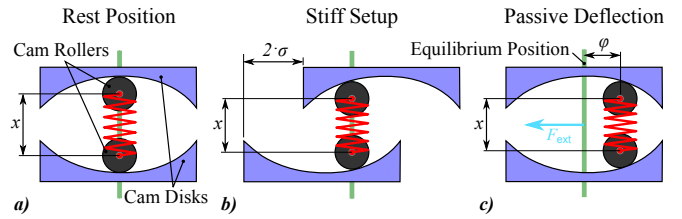


Fig. 8. BAVSdrive: Relative deflection between the cams causes compression of the spring that is located between the rollers. Each cam disk (shown in developed view) is connected to the circular spline of the HD. The wave generators are mounted on the output of the two motors. Thus, the output position without load equals the average of the positions of each flexspline/cam disk. In a) the mechanism is in rest position and in b) the equilibrium position in a stiff configuration is depicted. In c) the joint is deflected by an external torque.

torques for the forearm rotation and wrist actuation are higher than the ones for finger actuation. Furthermore, no tendons are used for actuation, which enables the use of the newly developed BAVS actuation (see II-A).

Similar to the FSJ, the mechanism consists of two opposing concave cams and two rollers preloaded by a linear spring (Fig. 8). The cam discs are symmetrical in both directions for BAVS actuation. An external load to the BAVS drive deflects both cam discs in the same direction. To change the compliance preset, the motors twist the cam disks in opposite direction, resulting in a larger spring load and an altered angle of contact between rollers and cams. This causes the non linear characteristics of the BAVS drive (Fig. 8).

The cam disks can be easily changed in order to test different stiffness-deflection relations.

D. Wrist

The desired motion range of the wrist and the expected tendon forces demand a special wrist design (Fig. 10). A roller guidance, which minimizes the tendon elongation during the wrist motion was developed. It keeps friction small and undesired centering forces from the hand tendons low. The wrist is based on the principle of an antiparallelogram (Fig. 9). Crossing bars held at base and end allow for a pivoting motion without changing their respective length. This principle was extended to a spherical antiparallelogram mechanism, which allows for $\pm 30^\circ$ sideways motion, as well as $\pm 90^\circ$ flexion/extension of the wrist. It is designed to withstand 6.5 kN, i.e. the sum of the maximum tendon forces. The wrist is actuated by 4 ServoModules.

E. Hand

The hand is the most exposed part of the robot, although it has the smallest force capabilities. The required features

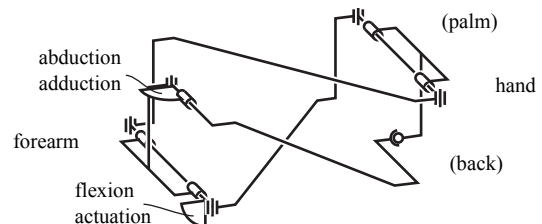


Fig. 9. Kinematics and actuation of the wrist.

are large dexterity, manipulation capabilities, and robustness against unwanted collisions. As the human hand is highly underactuated and uses several muscle/tendon synergies [25], which are not technically realizable, a plain copy of the human hand is not feasible. The hand design has to be based on an abstraction of the fundamental functionalities of the human hand. To reduce the number of drives, DoFs which have relatively low impact on grasping abilities should be omitted. These missing DoFs have to be compensated functionally by the kinematics design of the hand [20].

Overall, the kinematics of the new hand (Fig. 10) is closely adapted to the human hand on a functional basis [20]. It consists of 19 independent DoFs⁷ in order to reduce the number of necessary drives. Like human fingers the index and middle finger have 4 DoFs. The 2nd (PIP) and 3rd (DIP) finger joint⁸ of the ring and fifth finger are coupled to reduce the number of necessary actuators. The 5th DoF of the human thumb turned out to be of low relevance [26], [20] and has been omitted. To ensure proper opposition of the thumb and the 5th finger, an antagonistically driven 4 bar mechanism was designed to mimic the motion of the 5th finger metacarpal bone⁹.

The structure of the finger is designed as an endoskeleton with "bionic joints" [19]. The finger base (metacarpal) joint is a hyperboloidally shaped saddle joint because the human condyloid joint type can not be replicated technically¹⁰. The finger (interphalangeal) joints, on the other hand, are designed as hinge joints. All joints allow dislocation without damage in case of overload¹¹. In addition to robustness due to short-term energy storage, the use of antagonistic actuation (see II-A) enables to cope with tendon slackening or overstretching, which is one of the major problems of nowadays tendon-driven hands having inevitably constant tendon length. In contrast, antagonistic actuation is able to compensate unaligned pulley axes, and other geometrical errors via the elastic elements of the drive train. Therefore no explicit tendon tensioner is needed [18].

III. CONTROL

A precise modeling of the robot dynamics and the nonlinear adjustable stiffness mechanisms is compulsory to exploit the optimal performances of the systems. In this section, the control approaches are presented. The DLR Hand Arm System currently is divided into two subsystems, the arm subsystem and the wrist/hand subsystem, that are treated independently in order to facilitate the controller design.

A. Arm Control

The mechanical design goal for all joints is to achieve the desired stiffness characteristics precisely and with low friction to reduce hysteresis, resulting in a low intrinsic

⁷Thumb 4 DoF, index finger 4 DoFs, middle finger 4 DoFs, ringfinger 3 DoFs, 5th finger 4 DoFs

⁸starting from the fingers base

⁹the first bone of the finger located within the palm

¹⁰in a meaningful way

¹¹the elongation of the tendons in case of dislocation is compensated by the elastic elements of the antagonistic drives

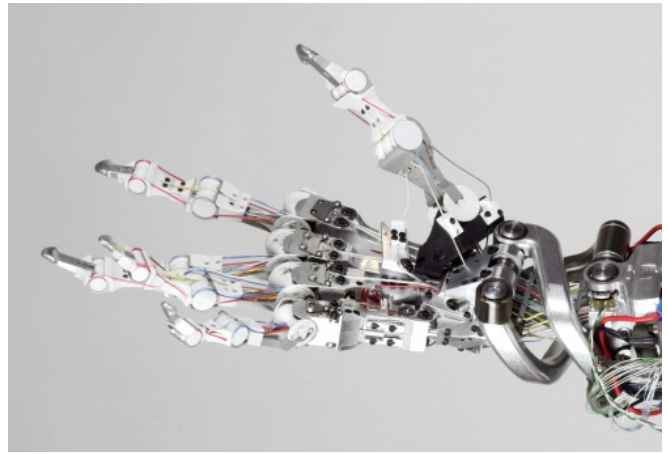


Fig. 10. Hand and wrist of the DLR Hand Arm System. Due to spacial restrictions, several sliding surfaces are used for the tendon routing. In order to ensure proper motion of the fingers even at high pretension, the palm design has to introduce minimal additional friction. Therefore, a palm design using ball bearing pulleys was realized (65 pulleys to route the tendons towards the fingers and 38 pulleys at the wrist interface).

damping. This property will especially be exploited to increase energy efficiency. However, in a motor position based control mode where the joint elasticity is not taken into account, large oscillations are likely to occur. Therefore, if a damped motion is required by the task, this has to be provided by active control. The joint elasticity together with the dynamic coupling between multiple joints of the robot arm pose a nonlinear, multi-input multi-output (MIMO) control problem.

A first damping control approach is presented in [27]. The idea is to perform a model based eigenmode decoupling for the linearized dynamics of the flexible joint model. In a first step, a torque feedback controller is used to shape the linearized system such that in a second step the eigenmode decoupling can be performed. This approach allows to transform the system into new coordinates in which the arm dynamics is decoupled. Well known single-input single-output control design tools are applied. Feedback controller gains are calculated such that the decoupled subsystems behave like well damped fourth order systems. After the final step of transforming the control gains back into the original coordinates, the arm is controlled by a state feedback control law. A sketch of the control approach is depicted in Fig. 11.

Several other controllers are tested on the system. For trajectory teaching, a torque controller with gravity compensation is used. This is a special case of a joint impedance controller with zero stiffness and feed forward gravity compensation.

Another controller under evaluation is the Cartesian impedance control algorithm adapted for the case of variable compliance. A focus lies on the combination of the active compliance provided by a controller and the passive compliance behavior of the VS joints.

B. Wrist/Hand Control

The major task of the wrist/hand control is to deal with the large number of actuators and its kinematic joint couplings.

A controller was designed that accepts the joint position and mechanical joint stiffness as input values using the properties of the antagonistic motor/tendon arrangement. However, the tendon routing does not allow for an arbitrary intrinsic stiffness matrix. To increase the compliance range an impedance controller is used in series with the progressive springs. The control scheme implemented on the system for the finger/wrist control is depicted in Fig. 12. It assumes that the singular perturbation hypothesis is holding. Therefore, the joint control and the tendon control are analyzed independently. The inputs of the impedance block are the reference joint trajectories and the current joint positions. According to the user defined impedance, it leads to the desired joint torques that can be mapped to the tendon forces (Fig. 12, B) by using the kinematic structure. The tendon forces are finally given as references to the underlying tendon force controller (Fig. 12, C). A kinematic model of the wrist is used to compensate for the tendon displacement due to motion of the wrist (Fig. 12, A). The controller must ensure a constant pulling constraint to avoid slack, and needs to prevent excessive force on the tendons (Fig. 12, D).

This controller represents a starting point from which a coordinated control architecture can be developed in order to fully exploit the system performances. For a more detailed description of other controllers please refer to [28].

IV. SOFTWARE

The robot operating software has to provide control designers with direct and convenient access to all robot functionalities, while retaining the necessary modularity. To satisfy the former, the interface to the robot control software is a Matlab Simulink block. A hardware abstraction layer (HAL) implements sensor value calibration and provides all relevant signals as SI-Units at the Simulink interface.

The challenges of distributed components, in particular synchronisation, scheduling, and error handling are met by the application of “The Virtual Path” component model [29]. “The Virtual Path” specifies modular components and a minimal control interface for distributed sensors, controllers, and actuators. Additionally, the signal-oriented middleware presented in [30] is used for the efficient integration of the distributed electronic components with the HAL Simulink

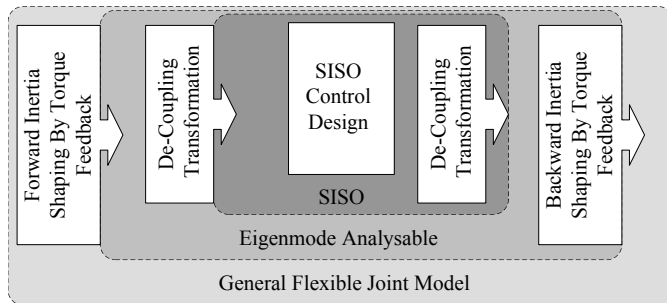


Fig. 11. The damping control algorithm consists of three main parts. First, torque feedback provides motor inertia shaping. This enables to use the eigenmode decoupling. Finally SISO control tools can be applied to ensure proper joint damping.

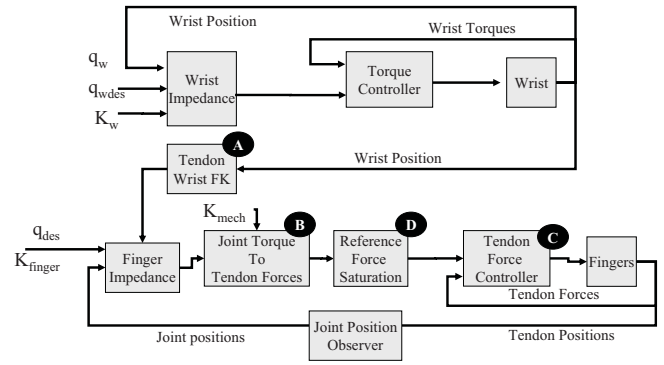


Fig. 12. Hand controller structure, the blocks marked with a letter are described in more details in the text (FK stands for forward kinematics).

block. Although a strict modularization is retained, the implementation achieves a 3 kHz control cycle at the Simulink interface. The typical overall delay for a single execution cycle, starting with sensor value acquisition, including one step Simulink calculation, to commanding the newly calculated values at the actuators is lower than 100 μ s.

V. ELECTRONICS

The electronics and system architecture design has to facilitate following major issues:

- reliability and maintainability
- communication and computation bandwidth
- power density and integration level

For this, we divided the system into highly integrated sub-components, which are self-contained and scalable modules. In particular, they enable the required flexibility, maintainability, and reliability. For such the DLR Hand Arm System is based on the application of the model based approach introduced in [29]. Furthermore, the large number of motors and sensors poses strong demands to communication bandwidth and a well structured communication concept. Therefore, a hierarchical solution is used, which features standardized protocol and physical connector interfaces.

Fig. 13 depicts the overall system communication topology. Actuators and sensors are connected via the standard industry BiSS bus. BiSS C-Mode is a serial reliable and bidirectional bus with very small footprint and a typical

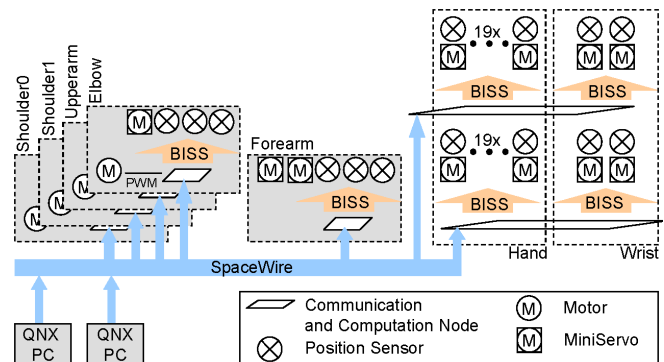


Fig. 13. Topology of the DLR Hand Arm System.

bandwidth of $10 \frac{Mbit}{s}$. Communication and control nodes aggregate data from the BiSS nodes and transmit it to real-time computing hosts via SpaceWire. SpaceWire [31] is a packet based bus with a bandwidth of up to $1 \frac{Gbit}{s}$ that is deterministic for a given topology.

In the following sections a short explanation of the key electronic components of DLR Hand Arm System is given.

1) *Power Supply*: Generally, careful design of power supply is a main prerequisite for such a complex mechatronic system¹². Hence, the special power supply unit IGOR was designed. IGOR is optimized for high peak power ratings, as well as the capability of brake power recuperation and comprises five separate switchable outputs with soft start and electronic fuses. Due to its banks of supercapacitors it is possible to provide 2 kW for one output or 4 kW in total for up to 1 s.

2) *Position Sensors*: As a consequence of the standardized interfaces described above, all sensors feature BiSS and the same connector. For the *flex sensors*¹³ a CPLD is used to read and transfer the digitized sensor data of the linear potentiometers. A custom-designed magneto-resistive sensor with a resolution of $23040 \frac{Incs}{rev}$, which is optimized for *hollow shaft drives*, is employed as the position sensor in the upperarm stack. The sensor used in the ILM25 Servo-Modules, IC-MH from IC-Haus, features $4096 \frac{Incs}{rev}$ and a very small volume consumption. The same sensor provides the deflection measurement of the "tan α mechanism" lever (Fig. 7) in the forearm. A special FEM designed magnet is optimized to cover the desired angle range and to enable the axial sensor to be used as an off-axis sensor.

3) *ILM25 ServoModules*: The motor module is a very compact self-contained intelligent component, which consists of a PMSM ILM25, inverter electronics, and control electronics (Fig. 14). The inverter electronics is directly mounted on the motor in order to keep power and position sensor connections as short as possible and to minimize EMI influences. A Xilinx Spartan 3e XC3S500EP132 with only 8x8 mm is responsible for communication (BiSS), as well as position and current control of the motor at 100 kHz. This high sampling rate is chosen due to the high dynamics of the motor as well as the need for low DC link ripples and small filter dimensions.

4) *Hand Electronics*: The forearm electronics comprises signal aggregation and routing. It is used as the SpaceWire communication backbone and is capable of connecting 26 BiSS modules. Two Virtex5 FPGA (V5LX50) provide the connection to the 26 BiSS masters, the SpaceWire links and routers, and the signal routing itself.

5) *Upperarm Stack*: The upperarm stack comprises two components: one power supply module and up to eight digital/inverter modules (Fig. 14). The digital/inverter module comprises the communication and computation capabilities described in V-4 combined with a fully integrated motor controller. The module provides a Virtex5 FPGA

¹²Just to give an idea, load alternations in the hand yield power consumption of more than 4 kW within a few milliseconds.

¹³measuring the deflection of the elastic elements

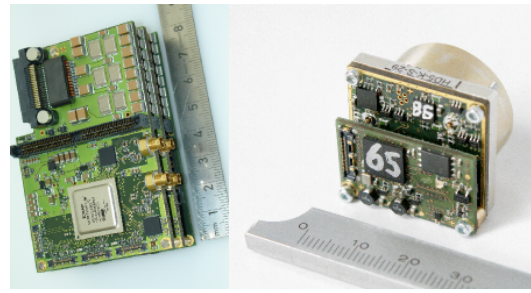


Fig. 14. Upperarm stack with one supply and 2 digital/inverter modules (left) and lowerarm drive module stack (right).

(V5LX50) as computation resource, two interfaces with $1 \frac{Gbit}{s}$ SpaceWire by using IEEE 802.3 physical layer, four interfaces with $100 \frac{Mbit}{s}$ for data exchange in between the stack modules, and 8 BiSS connectors.

VI. FIRST RESULTS

Impact tests have been performed to verify the robustness of the DLR Hand Arm System. E.g. the fingers of the hand have been hit with a 500 g hammer, while being in position control without any damage. As a first simple demonstration of the full system robustness a nail has been driven into wood (Fig. 15, attached video). The trajectory was taught and uses no sensory feedback.

Furthermore, the controller design has been evaluated doing experiments focused especially on multi DoF joint damping (see III). Long time exposure pictures of the undamped and damped system are shown in Fig. 16.

VII. CONCLUSION AND FUTURE WORKS

A highly integrated anthropomorphic hand arm system is presented. It was designed based on the analysis of the core functionalities of the human archetype in terms of robustness, dynamics, and dexterity. These capabilities were transferred to a robotic system using cutting edge robotic



Fig. 15. Sequence of the DLR Hand Arm System driving a nail into solid wood using a 500 g standard hammer.

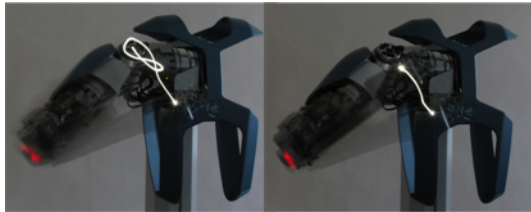


Fig. 16. Long time exposure pictures of the DLR Hand Arm System with a light source mounted at the TCP. On the left the damping control is switched off. The non-harmonic oscillatory and coupled motion can be seen. On the right the active damping control results in a very smooth TCP motion.

technologies. Variable stiffness actuation was identified as the key feature to overcome the strong limitations of nowadays robotic systems and aim for human-like performance. This is mainly due to the ability of VSA to dynamically store and release elastic energy, adjust the intrinsic joint stiffness online, and show high robustness properties against collisions with the environment. The DLR Hand Arm System unifies human-like dynamic properties into a compact design and has already shown its high robustness and dynamic capabilities in some initial experiments. Its robustness is also thought to enable application engineers to concentrate on the development of new control and planning methods, rather than on avoiding collisions and possibly resulting hardware defects¹⁴ during testing phase.

VIII. ACKNOWLEDGMENT

The authors would like to thank J. Böhne, B. Bohnhorst, Ch. Borst, M. Brey, H. Buchner, M. Dreier, P. Ebner, F. Hacker, B. Hartmann, M. Heumos, K. Jöhl, J. Langwald, M. Leichtenstern, G. Passig, B. Pleintinger, A. Regner, M. Schedl, P. vd. Smagt, G. Stillfried, M. Sündermann, T. v. Tran, H. Wagner and F. Zacharias for their contributions to the DLR Hand Arm System as well as Adalbert Kapandji for his great explanations of the human hand.

This work is partly funded by the EU grant STIFF (FP7-ICT-231576) and VIATORS (FP7-ICT-2007-3).

REFERENCES

- [1] B. Bäuml, T. Wimböck, and G. Hirzinger, "Kinematically optimal catching a flying ball with a hand-arm-system," in *Proc. IEEE/RSJ International Conf. on Intelligent Robots and Systems (IROS)*, 2010, pp. 2592–2599.
- [2] Y. Sakagami, R. Watanabe, C. Aoyama, S. Matsunaga, N. Higaki, and K. Fujimura, "The intelligent ASIMO: System overview and integration," in *Proc. IEEE/RSJ International Conf. on Intelligent Robots and Systems (IROS)*, 2002, pp. 2478–2483.
- [3] K. Kaneko, F. Kanehiro, S. Kajita, K. Yokoyama, K. Akachi, T. Kawasaki, S. Ota, and T. Isozumi, "Design of prototype humanoid robotics platform for HRP," in *Proc. IEEE/RSJ International Conf. on Intelligent Robots and Systems (IROS)*, 2002, pp. 2431–2436.
- [4] T. Morita, H. Iwata, and S. Sugano, "Development of human symbiotic robot: WENDY," in *Proc. IEEE International Conf. on Robotics and Automation (ICRA)*, 1999, pp. 3183–3188.
- [5] H. Iwata and S. Sugano, "Design of human symbiotic robot twenty-one," in *Proc. IEEE International Conf. on Robotics and Automation (ICRA)*, may 2009, pp. 580–586.
- [6] M. Diftler, J. Mehling, M. Abdallah, N. Radford, L. Bridgwater, A. Sanders, S. Askew, D. Linn, J. Yamokoski, F. Permenter, B. Hargrave, R. Platt, R. Savely, and R. Ambrose, "Robonaut 2: The first humanoid robot in space," in *Proc. IEEE International Conf. on Robotics and Automation (ICRA)*, 2011.
- [7] I. Mizuuchi, R. Tajima, T. Yoshikai, D. Sato, K. Nagashima, M. Inaba, Y. Kuniyoshi, and H. Inoue, "The design and control of the flexible spine of a fully tendon-driven humanoid "kenta"," in *Proc. IEEE/RSJ International Conf. on Intelligent Robots and Systems (IROS)*, 2002.
- [8] I. Mizuuchi, Y. Nakanishi, Y. Sodeyama, Y. Namiki, T. Nishino, N. Muramatsu, J. Urata, K. Hongo, T. Yoshikai, and M. Inaba, "An advanced musculoskeletal humanoid kojiro," in *Proc. IEEE-RAS International Conference on Humanoid Robots (HUMANOIDS)*, 2007.
- [9] Y. Matsuoka, P. Afshar, and M. Oh, "On the design of robotic hands for brain-machine interface," *Neurosurgical focus*, vol. 20, no. 5, pp. 1–9, 2006.
- [10] K. Laurin-Kovitz, J. Colgate, and S. Carnes, "Design of programmable passive impedance," in *Proc. IEEE International Conf. on Robotics and Automation (ICRA)*, 1991, pp. 1476–1481.
- [11] C. English and D. Russell, "Implementation of variable joint stiffness through antagonistic actuation using rolamite springs," *Mechanism and Machine Theory*, vol. 34, no. 1, pp. 27–40, 1999.
- [12] G. Palli, C. Melchiorri, T. Wimbock, M. Grebenstein, and G. Hirzinger, "Feedback linearization and simultaneous stiffness-position control of robots with antagonistic actuated joints," in *Proc. IEEE International Conf. on Robotics and Automation (ICRA)*, Apr. 2007, p. 4367–4372.
- [13] S. Wolf and G. Hirzinger, "A new variable stiffness design: Matching requirements of the next robot generation," in *Proc. IEEE International Conf. on Robotics and Automation (ICRA)*, 2008, p. 1741–1746.
- [14] R. Schiavi, G. Grioli, S. Sen, and A. Bicchi, "VSA-II: a novel prototype of variable stiffness actuator for safe and performing robots interacting with humans," in *Proc. IEEE International Conf. on Robotics and Automation (ICRA)*, May 2008, p. 2171–2176.
- [15] A. Albu-Schäffer, C. Ott, and G. Hirzinger, "A unified passivity based control framework for position, torque and impedance control of flexible joint robots," *International Journal of Robotics Research*, vol. 26, no. 1, pp. 23 – 39, Jan. 2007.
- [16] S. Haddadin, A. Albu-Schäffer, and G. Hirzinger, "Safety evaluation of physical human-robot interaction via crash-testing," in *Proc. Robotics: science and systems conference (RSS)*, 2007, p. 217–224.
- [17] S. Haddadin, A. Albu-Schäffer, O. Eiberger, and G. Hirzinger, "New insights concerning intrinsic joint elasticity for safety," in *Proc. IEEE/RSJ International Conf. on Intelligent Robots and Systems (IROS)*, Taipei, Taiwan, 2010, pp. 2181–2187.
- [18] M. Grebenstein and P. van der Smagt, "Antagonism for a highly anthropomorphic HandArmSystem," *Advanced Robotics*, no. 22, pp. 39 – 55, 2008.
- [19] M. Grebenstein, M. Chalon, G. Hirzinger, and R. Siegwart, "Antagonistically driven finger design for the anthropomorphic DLR hand arm system," in *Proc. IEEE-RAS International Conference on Humanoid Robots (HUMANOIDS)*, 2010.
- [20] —, "A method for hand kinematics designers; 7 billion perfect hands," in *Proc. International Conference on Applied Bionics and Biomechanics (ICABB)*, 2010.
- [21] S. Wolf, O. Eiberger, and G. Hirzinger, "The DLR FSJ: energy based design of a variable stiffness joint," in *Proc. IEEE International Conf. on Robotics and Automation (ICRA)*, 2011.
- [22] M. Grebenstein, "Antagonistische Schwenkvorrichtung," German Patent Request DE 10 2006 016 958 A1, jan. 2006.
- [23] F. Petit, M. Chalon, W. Friedl, M. Grebenstein, A. Albu-Schäffer, and G. Hirzinger, "Bidirectional antagonistic variable stiffness actuation: Analysis, design and implementation," in *Proc. IEEE International Conf. on Robotics and Automation (ICRA)*, May 2010, pp. 4189 –4196.
- [24] O. Eiberger, S. Haddadin, M. Weis, A. Albu-Schäffer, and G. Hirzinger, "On joint design with intrinsic variable compliance: derivation of the DLR QA-Joint," in *Proc. IEEE International Conf. on Robotics and Automation (ICRA)*, 2010, p. 1687–1694.
- [25] H. Gray, *Anatomy, descriptive and surgical*. Philadelphia: Courage Books, 1999.
- [26] M. Chalon, M. Grebenstein, T. Wimboeck, and G. Hirzinger, "The thumb: Guidelines for a robotic design," in *Proc. IEEE/RSJ International Conf. on Intelligent Robots and Systems (IROS)*, 2010.
- [27] F. Petit and A. Albu-Schäffer, "State feedback damping control for a multi DOF variable stiffness robot arm," in *Proc. IEEE International Conf. on Robotics and Automation (ICRA)*, 2011.
- [28] T. Wimböck, Ch. Ott, A. Albu-Schäffer, A. Kugi, and G. Hirzinger, "Impedance control for variable stiffness mechanisms with nonlinear joint coupling," in *Proc. IEEE/RSJ International Conf. on Intelligent Robots and Systems (IROS)*, 2008, pp. 3796–3803.
- [29] M. Nickl, S. Jörg, and G. Hirzinger, "The virtual path: The domain model for the design of the MIRO surgical robotic system," in *9th International IFAC Symposium on Robot Control, IFAC*. Gifu, Japan: <http://www.ifac-papersonline.net/>, 2009, pp. 97–103.
- [30] S. Jörg, M. Nickl, and G. Hirzinger, "Flexible signal-oriented hardware abstraction for rapid prototyping of robotic systems," in *Proc. IEEE/RSJ International Conf. on Intelligent Robots and Systems (IROS)*, Beijing, Oct. 2006, pp. 3755 – 3760.
- [31] E. C. for Space Standardization (ECSS), "SpaceWire - links, nodes, routers and networks eCSS E-50-12A," 2003.

¹⁴methods as e.g. reinforcement learning actually rely on collisions to succeed in learning also the dynamics of contact with the physical world